ARMY RESEARCH LABORATORY

Simulation of Mass Transfer Process for Polymer Electrolyte Membrane Fuel Cell Stack

Deryn Chu and Rongzhong Jiang

ARL-TR-2086

February 2000

Army Research Laboratory

Adelphi, MD 20783-1197

ARL-TR-2086 **February 2000**

Simulation of Mass Transfer Process for Polymer Electrolyte Membrane Fuel Cell Stack

Deryn Chu and Rongzhong Jiang
Sensors and Electron Devices Directorate

Abstract

We propose an empirical equation to simulate the potential-current and power-current curves for a polymer electrolyte membrane fuel cell (PEMFC) stack. The equation has been demonstrated to fit experimental curves excellently for the entire reaction process, including activation, ohmic, and mass-transfer controls. Using this equation to simulate the mass-transfer process will not cause different results for the E_o, b, and R values than using the analytical equation ($E_i = E_o - b \log i - Ri$). The effect of each mass-transfer parameter on the shape of the potential-current and power-current curves are compared, and overall they show a regular variation. We also analyzed the effect of relative humidity on the performance of a strip design PEMFC stack.

Contents

1. Introduction 1
2. Development of the Model 1
3. Simulation by Varying Mass-Transfer Parameters 3
4. Simulation of Experimental Curves 5
5. Summary 6
Acknowledgment 6
References 7
Distribution 9
Report Documentation Page 11

Figures

1. Typical potential-current behavior of 10-cell PEMFC stack with mass-transfer limitation 2
2. Effect of n value on model of 10-cell PEMFC stack's potential- and power-current curves (E_o = 10 V, b = 600 mV/dec, R = 0.5 Ω, i_d = 1.44 A, and m = 0.1 Ω); n values vary from bottom to top curves as 3.0, 1.5, 0.5, and 0.2 A^{-1}, respectively 4
3. Effect of i_d value on model of 10-cell stack PEMFC's potential- and power-current curves (E_o = 10 V, b = 600 mV, R = 0.5 Ω, m = 0.1 Ω, and n = 1.5 A^{-1}); i_d values vary from bottom to top curves as 0.83, 1.44, 2.2, and 3.0, respectively 4
4. Effect of m value on model of 10-cell PEMFC stack's potential- and power-current curves (E_o = 10 V, b = 600 mV/dec, R = 0.5 Ω, i_d = 1.44 A, and n = 1.5 A^{-1}); m values vary from bottom to top curves as 1.0, 0.5, 0.1, and 0.01 Ω, respectively 4
5. Experimental curve simulation for strip design 10-cell PEMFC stack at different humidities 5
6. Plot of mass-transfer impedance versus stack current at different humidity levels 6

Table

1. Electrode-kinetic and mass-transfer parameters for strip PEMFC stack at different humidity levels 5

1. Introduction

A polymer electrolyte membrane fuel cell (PEMFC) is one of the best candidates for a portable power supply device for commercial applications, primarily because it is lightweight and has a high power density. Much attention has been given to PEMFC research and development during the last 10 years [1–10]. Most research has concentrated on single PEMFCs. However, PEMFC stacks have recently been developed with a variety of designs and different applications [11–14]. The performance of a PEMFC stack is different from that of a single PEMFC. In our investigation of the PEMFC stack, we observed mass-transfer phenomena when the stack was operating at high current density. This is probably because of low oxygen concentration, slow heat dispersion, and improper water management, especially for an air-breathing PEMFC stack. To reach a high power density, the PEMFC stack must operate under conditions that require a high current density, such as being a power source in an electric vehicle.

An understanding of the electrode processes of mass transfer is important in designing and constructing a PEMFC stack. Since the early 1960s, several modeling studies have been conducted to explain single-cell potential versus current density behavior [5 and references therein]. However, analytic expressions for the potential-current behavior have been developed only in special cases, such as when electrode reactions are either activation and ohmic or activation and mass-transfer controlled. When all forms of overpotentials (activation, ohmic, and mass transfer) are present, as at high current density, there are no analytical solutions for the second-order differential equations. Kim et al [5] have reported mass-transfer phenomena in single-cell PEMFC and modeled the potential-current behaviors with an empirical equation, which shows excellent fit with the experimental potential-current curves. However, their equation gives different values of kinetic parameters (E_o, b, and R) when a convenient analytical equation is used alone (for activation and ohmic control). In this report, we simulate the mass-transfer behavior for a PEMFC stack with a modified empirical equation to obtain the same kinetic values as when using a convenient analytical equation.

2. Development of the Model

Figure 1 shows a typical potential-current curve of a 10-cell strip air-breathing PEMFC stack. We obtained the points in the figure from experimental data. When the current is high enough, the experimental points drop quickly to a zero-voltage value. As is well known, electrode processes can be attributed to activation, ohmic, and mass-transfer controls. Activation occurs mainly at the beginning of the potential-current curve, ohmic control at the middle, and mass transfer at the high current density

Figure 1. Typical potential-current behavior of 10-cell PEMFC stack with mass-transfer limitation. Points were obtained from experiment. Lines are calculated curves with equations (1) and (6), respectively.

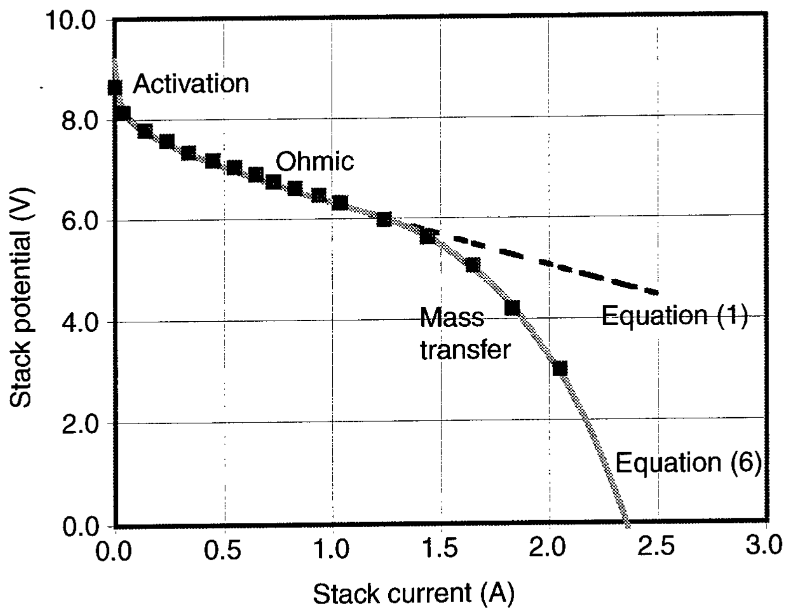

ranges. The potential-current behavior at the low and middle current ranges can be described as [5,6]

$$E_i = E_o - b \log i - Ri \ , \tag{1}$$

where

$$E_o = E_r + b \log i_o \ . \tag{2}$$

In these equations, E_i (V) and i (A) are the experimentally measured potential and current, E_r (V) is the reversible potential for the stack, and i_o (A) and b (mV/dec) are the exchange current and the Tafel slope for the oxygen reduction, respectively. R (Ω) represents the direct current resistance, such as the resistance in the polymer membrane and other stack components, that causes a linear variation of potential with the current. The top curve (dashed line) in figure 1 is calculated with equation (1), which deviates from the experimental points at higher current density ranges. However, the curve calculated with equation (1) gives a good fit with the experimental data only at the low and middle current density ranges.

The entire current range of the potential-current curve can be described as

$$E_i = E_o - b \log i - Ri - \Delta E \ , \tag{3}$$

where ΔE (V) is the overpotential caused by mass transfer.

An expression has been developed for ΔE by Rho et al [6]:

$$\Delta E = m \exp(ni) \ . \tag{4}$$

Combining equations (1) and (4) gives

$$E_i = E_o - b \log i - Ri - m \exp(ni) \ . \tag{5}$$

The m and n in equations (4) and (5) are mass-transfer parameters [5]. With equation (5), we have demonstrated an excellent fit with the experimental data in the presence of mass transfer. However, using equation (5) gives different values of E_o, b, and R than does using equation (1). We developed an equation that can give the same values of E_o, b, and R with equation (1) in the entire current range. We did this by modifying equation (5):

$$E_i = E_o - b \log i - Ri - i_m m \exp(n i_m) \ , \tag{6}$$

$$i_m = i - i_d \text{ (when } i > i_d\text{), and} \tag{7}$$

$$i_m = 0 \text{ (when } i \leq i_d\text{)} \ . \tag{8}$$

In equations (7) and (8), i_d (A) is the minimum value of current that causes the voltage deviation from the linearity in figure 1. The i_d value can be obtained from the experimental curve and from the calculated curve with equation (1). The m (Ω) and n (A^{-1}) are the mass-transfer parameters (their definitions are somewhat different from ref. 5), which describe the second slope of potential decrease with current and the degree of curvature at the stack's polarization curve in the high current density range, respectively. The i_m (A) is mass transfer current; its meaning is defined by equation (7).

Equation (6) gives an excellent fit with the potential-current curves in the entire range of current. For instance, the bottom curve (solid line) shown in figure 1 was calculated with equation (6), which agrees with the experimental points. The two lines in figure 1 were both calculated with equations (1) and (6) and give the same values of E_o, b, and R.

3. Simulation by Varying Mass-Transfer Parameters

To better understand equation (6), we investigated the three parameters i_d, m, and n. We kept the E_o, b, and R values constant and varied the i_d, m, or n values one by one. Figure 2 shows the effect of the n parameter on the potential-current and power-current curves. When the n value decreases, the potential-current curve becomes less curved, and gradually becomes a straight line when the n value is close to zero; also the power-current curve becomes a large arch, and the peak power at $n = 0.2\ A^{-1}$ almost doubles that at $n = 3.0\ A^{-1}$. Figure 3 shows the effect of the i_d parameter on the potential-current and power-current curves. The curvature of the potential-current curve has no significant change with the increase of i_d. However, the start point, where deviation from equation (1) occurs, is moving to a higher current value. The power-current curve exhibits an asymmetrical arch, and its peak power increases with the addition of the i_d value. Figure 4 shows the effect of the m parameter on the potential-current and power-current curves. The m parameter does not affect the curvature of the potential-current curve, but it increases the slope with an increase of the m number. The power-current curve is also shown as an arch, and the peak power increases with a decrease of the m number.

Figure 2. Effect of n value on model of 10-cell PEMFC stack's potential- and power-current curves (E_o = 10 V, b = 600 mV/dec, R = 0.5 Ω, i_d = 1.44 A, and m = 0.1 Ω); n values vary from bottom to top curves as 3.0, 1.5, 0.5, and 0.2 A^{-1}, respectively.

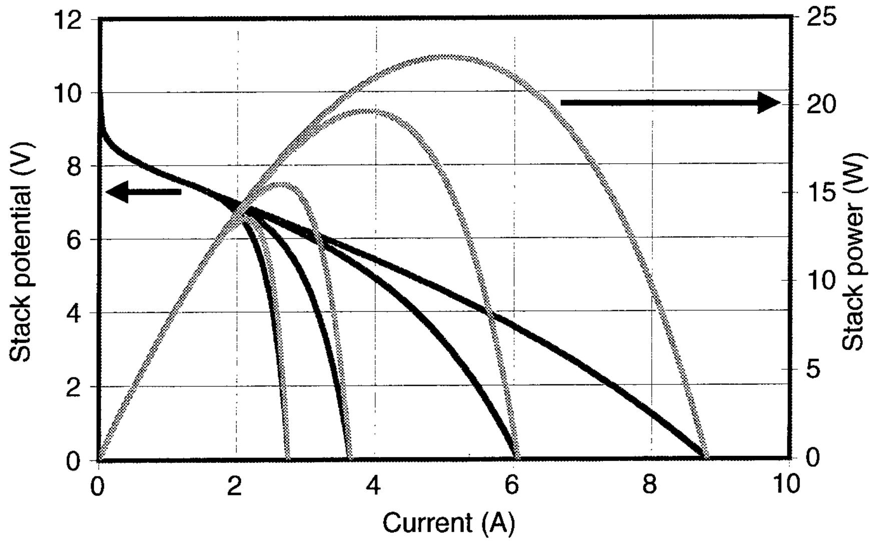

Figure 3. Effect of i_d value on model of 10-cell PEMFC stack's potential- and power-current curves (E_o = 10 V, b = 600 mV, R = 0.5 Ω, m = 0.1 Ω, and n = 1.5 A^{-1}); i_d values vary from bottom to top curves as 0.83, 1.44, 2.2, and 3.0, respectively.

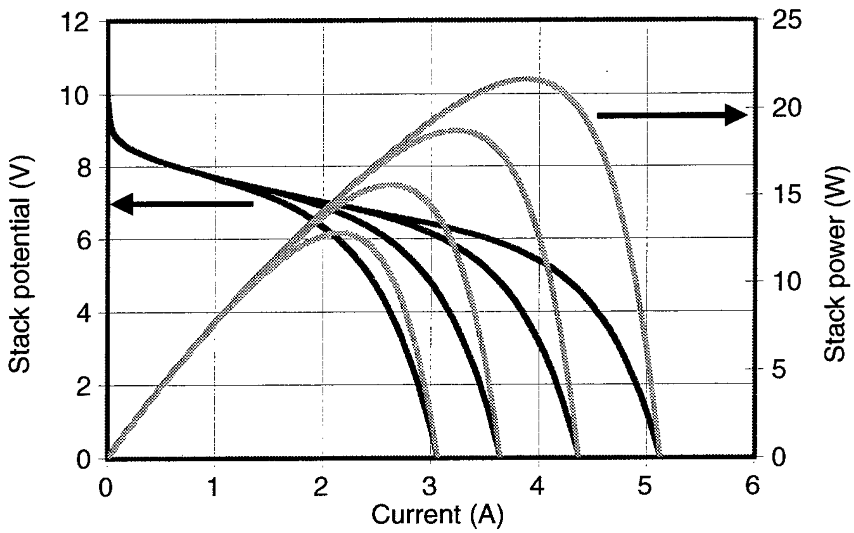

Figure 4. Effect of m value on model of 10-cell PEMFC stack's potential- and power-current curves (E_o = 10 V, b = 600 mV/dec, R = 0.5 Ω, i_d = 1.44 A, and n = 1.5 A^{-1}); m values vary from bottom to top curves as 1.0, 0.5, 0.1, and 0.01 Ω, respectively.

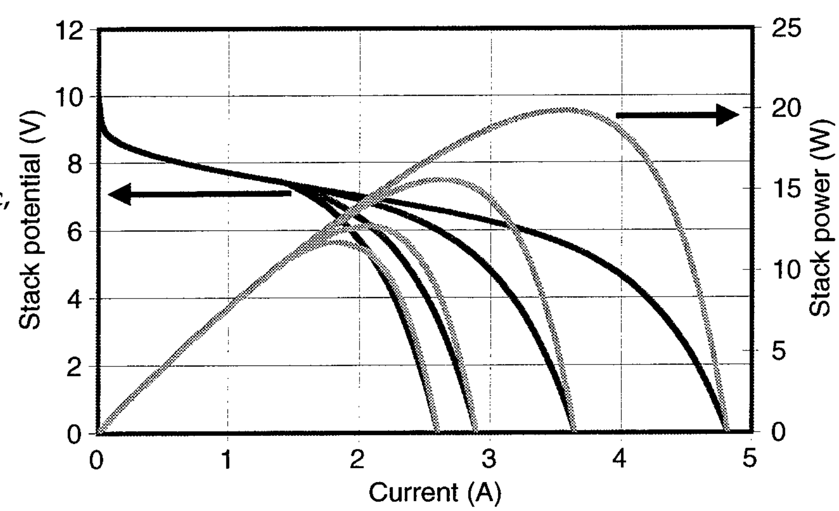

4. Simulation of Experimental Curves

Figure 5 shows the potential-current and power-current curves for a strip PEMFC stack operating at different humidity levels. The points on the curves were obtained from experimental data, and the lines were calculated with equation (6). When the humidity decreases, the curves apparently bend down, which implies that the mass-transfer controlled process becomes more serious at a low humidity. The power-current curve first increases and then decreases with current. Therefore, peak power values are formed. For conditions with 90 and 70 percent relative humidity, the maximum powers are 8.3 and 6.5 W, respectively. The kinetic parameters are obtained from the computer fitting and are listed in table 1. When the humidity increases, the b and R values both decrease, but the i_d value increases. The n value is kept constant during each calculation. The m and n parameters seem difficult to compare when they have different i_d values. However, we can solve this problem by comparing another kinetic parameter, mass-transfer impedance (R_m (Ω)), which is defined as

$$R_m = \Delta E / i = (i_m m \exp(n i_m)) / i \ . \qquad (9)$$

In our study, we only used the m and n parameters to obtain the optimum fit with the experimental points and used equation (9) to calculate the mass-transfer impedance beyond the range of experimental data. Figure 6

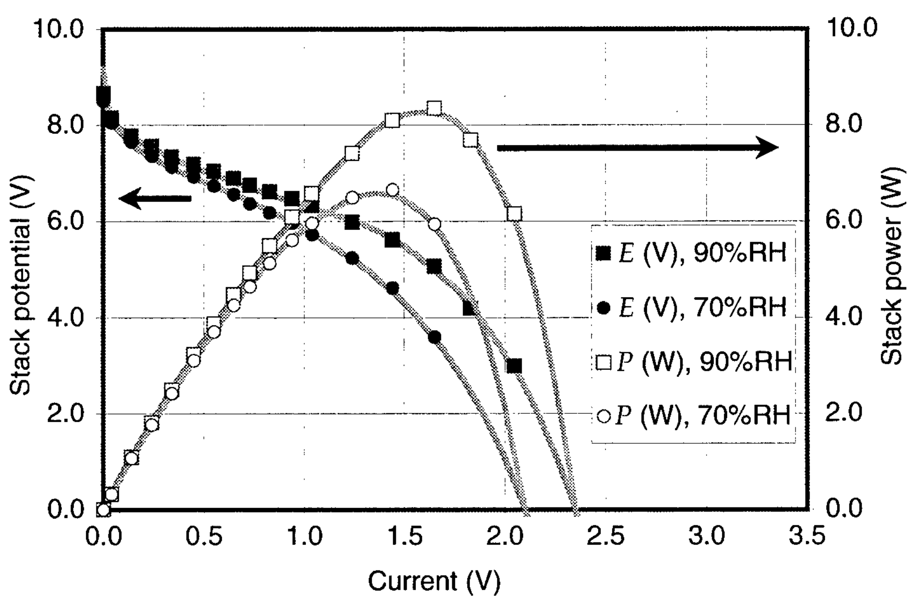

Figure 5. Experimental curve simulation for strip design 10-cell PEMFC stack at different humidities. Temperature constant at 30 °C. Points and lines are experimental data and computer-calculated curves, respectively.

Table 1. Electrode-kinetic and mass-transfer parameters for strip PEMFC stack at different humidity levels. Temperature is constant at 30 °C.

% RH	E_o (V)	b (mV/dec)	R (Ω)	m (Ω)	n (A^{-1})	i_d (A)
70	9.2	680	1.1	0.36	1.5	0.65
90	9.2	600	1.08	1.0	1.5	1.34

Figure 6. Plot of mass-transfer impedance versus stack current at different humidity levels. Temperature constant at 30 °C.

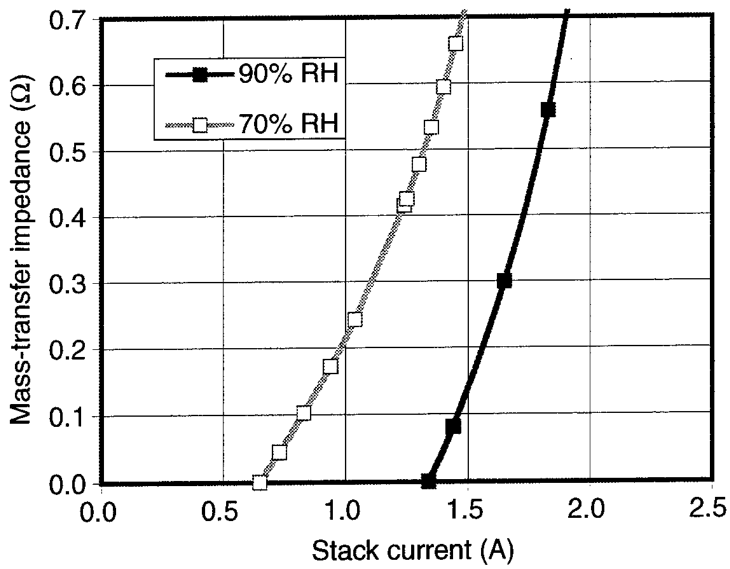

shows the calculated mass-transfer impedance for conditions with 70 and 90 percent relative humidity. The lower humidity has a much larger mass-transfer impedance. The mass-transfer impedance starts at zero and increases quite quickly with current for both humidity levels.

5. Summary

We proposed an empirical equation (eq (6)) to describe the entire reaction process of a PEMFC stack, including activation, ohmic, and mass-transfer controls. This equation demonstrated an accurate fit with experimental potential-current curves without causing different kinetic values of E_o, b, and R with that of using the analytical equation (eq (1)). The effect of each mass-transfer parameter (m, n, and i_d) on the change of the shape of the potential-current and power-current curves was compared, and overall they showed a regular variation. The experimental potential-current and power-current curves at different humidity levels were simulated, and a series of kinetic and mass-transfer parameters were obtained by the simulation. We defined a concept of mass-transfer resistance (R_m), and analyzed the variation of mass-transfer resistance with current at different humidity levels.

Acknowledgment

The authors wish to thank the U.S. Army Materiel Command (AMC) for its financial support of this project.

References

1. T. F. Fuller, "Is a Fuel Cell in Your Future?" *The Electrochemical Society Interface* (Fall 1997), p 26.
2. E. A. Ticianelli, C. R. Derouin, and S. Srinivasan, "Localization of Platinum in Low Catalyst Loading Electrodes to Attain High Power Density in SPE Fuel Cells," *J. Electroanal. Chem.* **251** (1988), p 175.
3. I. D. Raistrick, "Electrode Assembly for Use in a Solid Polymer Electrolyte Fuel Cell," U.S. patent No. 4,876,115 (1990).
4. M. S. Wilson and S. Gottesfeld, "Thin-Film Catalysis Layers for Polymer Electrolyte Fuel Cell Electrodes," *J. Appl. Electrochem.* **22** (1992), pp 1–7.
5. J. Kim, S. M. Lee, S. Srinivasan, and C. E. Chamberlin, "Modeling of Proton Exchange Membrane Fuel Cell Performance with an Empirical Equation," *J. Electrochem. Soc.* **142** (1995), p 2670.
6. Y. W. Rho, O. A. Velev, S. Srinivasan, and Y. T. Kho, "Mass Transfer Phenomena in Proton Exchange Membrane Fuel Cells Using O_2/He, O_2/Ar, and O_2/N_2 Mixtures, I. Experimental Analysis," *J. Electrochem. Soc.* **141** (1994), p 2084.
7. H. F. OetJen, V. M. Schmidt, U. Stimming, and F. Trila, "Performance Data of a Proton Exchange Membrane Fuel Cell Using H_2/CO as Fuel Gas," *J. Electrochem. Soc.* **143** (1996), p 3838.
8. M. Uchida, Y. Aoyama, N. Eda, and A. Ohta, "Investigation of the Microstructure in the Catalyst Layer and Effects of Both Perfluorosulfonate Ionomer and PTFE-Loaded Carbon on the Catalyst Layer of Polymer Electrolyte Fuel Cells," *J. Electrochem. Soc.* **142** (1995), p 4143.
9. F. N. Buchi, B. Gupta, O. Haas, and G. G. Scherer, "Performance of Differently Cross-Linked, Partially Fluorinated Proton Exchange Membranes in Polymer Electrolyte Fuel Cells," *J. Electrochem. Soc.* **142** (1995), p 3044.
10. M. Uchida, Y. Aoyama, N. Eda, and A. Ohta, "New Preparation Method for Polymer-Electrolyte Fuel Cells," *J. Electrochem. Soc.* **142** (1995), p 463.
11. J. B. Lakeman and J. Cruickshank, "A Lightweight Ambient Air Breathing Fuel Cell Stack," *Proceedings of the 38th Power Sources Conference*, Cherry Hill, NJ (June 1998), p 420.
12. A. Cisar, O. J. Murphy, and E. Clarke, "Low-Cost, Lightweight, High Power Density PEM Fuel Cell Stack," *Proceedings of the 38th Power Sources Conference*, Cherry Hill, NJ (June 1998), p 424.
13. L. P. Jarvis and D. Chu, "The Electrochemical Performance of a 100-Watt Polymer Electrolyte Membrane Fuel Cells and Single Cells," *Proceedings of the 38th Power Sources Conference*, Cherry Hill, NJ (June 1998), p 428.
14. O. Polevaya and D. Bloomfield, "Performance Modeling in a Lightweight Fuel Cell Stack," *Proceedings of the 38th Power Sources Conference*, Cherry Hill, NJ (June 1998), p 416.

Distribution

Admnstr
Defns Techl Info Ctr
Attn DTIC-OCP
8725 John J Kingman Rd Ste 0944
FT Belvoir VA 22060-6218

Ofc of the Secy of Defns
Attn ODDRE (R&AT)
The Pentagon
Washington DC 20301-3080

OSD
Attn OUSD(A&T)/ODDR&E(R) R J Trew
Washington DC 20301-7100

Advry Grp on Elect Devices
Attn Documents
Crystal Sq 4 1745 Jefferson Davis Hwy Ste 500
Arlington VA 22202

AMCOM MRDEC
Attn AMSMI-RD W C McCorkle
Redstone Arsenal AL 35898-5240

CECOM
Attn PM GPS COL S Young
FT Monmouth NJ 07703

CECOM Night Vsn/Elect Sensors Dirctrt
Attn AMSEL-RD-NV-D
FT Belvoir VA 22060-5806

Commander
CECOM R&D
Attn AMSEL-IM-BM-I-L-R Stinfo Ofc
Attn AMSEL-IM-BM-I-L-R Techl Lib
FT Monmouth NJ 07703-5703

Deputy for Sci & Techlgy
Attn Ofc Asst Sec Army (R&D)
Washington DC 30210

Dir for MANPRINT
Ofc of the Deputy Chief of Staff for Prsnnl
Attn J Hiller
The Pentagon Rm 2C733
Washington DC 20301-0300

Hdqtrs
Attn DAMA-ARZ-D F D Verderame
Washington DC 20310

TECOM
Attn AMSTE-CL
Aberdeen Proving Ground MD 21005-5057

US Army Armament Rsrch Dev & Engrg Ctr
Attn AMSTA-AR-TD M Fisette
Bldg 1
Picatinny Arsenal NJ 07806-5000

Commander
US Army CECOM
Attn AMSEL-RD-CZ-PS-B M Brundage
FT Monmouth NJ 07703-5000

US Army CECOM Rsrch Dev & Engrg Ctr
Attn AMSEL-RD-AS-BE E Plichta
FT Monmouth NJ 07703-5703

US Army Edgewood RDEC
Attn SCBRD-TD G Resnick
Aberdeen Proving Ground MD 21010-5423

US Army Info Sys Engrg Cmnd
Attn ASQB-OTD F Jenia
FT Huachuca AZ 85613-5300

US Army Natick RDEC
Acting Techl Dir
Attn SSCNC-T P Brandler
Natick MA 01760-5002

US Army Simulation, Train, & Instrmntn Cmnd
Attn J Stahl
12350 Research Parkway
Orlando FL 32826-3726

US Army Tank-Automtv Cmnd Rsrch, Dev, & Engrg Ctr
Attn AMSTA-TA J Chapin
Warren MI 48397-5000

Distribution (cont'd)

US Army Train & Doctrine Cmnd
Battle Lab Integration & Techl Dirctrt
Attn ATCD-B J A Klevecz
FT Monroe VA 23651-5850

US Military Academy
Mathematical Sci Ctr of Excellence
Attn MDN-A LTC M D Phillips
Dept of Mathematical Sci Thayer Hall
West Point NY 10996-1786

Nav Rsrch Lab
Attn Code 2627
Washington DC 20375-5000

Nav Surface Warfare Ctr
Attn Code B07 J Pennella
17320 Dahlgren Rd Bldg 1470 Rm 1101
Dahlgren VA 22448-5100

Marine Corps Liaison Ofc
Attn AMSEL-LN-MC
FT Monmouth NJ 07703-5033

USAF Rome Lab Tech
Attn Corridor W Ste 262 RL SUL
26 Electr Pkwy Bldg 106
Griffiss AFB NY 13441-4514

DARPA
Attn S Welby
3701 N Fairfax Dr
Arlington VA 22203-1714

Hicks & Associates Inc
Attn G Singley III
1710 Goodrich Dr Ste 1300
McLean VA 22102

Palisades Inst for Rsrch Svc Inc
Attn E Carr
1745 Jefferson Davis Hwy Ste 500
Arlington VA 22202-3402

Army Rsrch Ofc
Attn AMSRL-RO-EN Bach
Attn AMSRL-RO-EN B Mann
Attn AMSRL-RO-D JCI Chang
PO Box 12211
Research Triangle Park NC 27709

US Army Rsrch Lab
Attn AMSRL-DD J Miller
Attn AMSRL-CI-AS Mail & Records Mgmt
Attn AMSRL-CI-AT Techl Pub (3 copies)
Attn AMSRL-CI-LL Techl Lib (3 copies)
Attn AMSRL-SE-D E Scannell
Attn AMSRL-SE-DC D Chu (30 copies)
Attn AMSRL-SE-DC S Gilman
Attn AMSRL-SE-E J Mait
Adelphi MD 20783-1197

REPORT DOCUMENTATION PAGE

Form Approved
OMB No. 0704-0188

1. AGENCY USE ONLY *(Leave blank)*	2. REPORT DATE	3. REPORT TYPE AND DATES COVERED
	February 2000	Progress, Oct. 1998 to Sept. 1999

4. TITLE AND SUBTITLE Simulation of Mass Transfer Process for Polymer Electrolyte Membrane Fuel Cell Stack

5. FUNDING NUMBERS
DA PR: N/A
PE: 62120A

6. AUTHOR(S) Deryn Chu and Rongzhong Jiang

7. PERFORMING ORGANIZATION NAME(S) AND ADDRESS(ES)
U.S. Army Research Laboratory
Attn: AMSRL-SE-DC email: dchu@arl.mil
2800 Powder Mill Road
Adelphi, MD 20783-1197

8. PERFORMING ORGANIZATION REPORT NUMBER
ARL-TR-2086

9. SPONSORING/MONITORING AGENCY NAME(S) AND ADDRESS(ES)
U.S. Army Research Laboratory
2800 Powder Mill Road
Adelphi, MD 20783-1197

10. SPONSORING/MONITORING AGENCY REPORT NUMBER

11. SUPPLEMENTARY NOTES
ARL PR: 9NV4VV
AMS code: 622120.H16

12a. DISTRIBUTION/AVAILABILITY STATEMENT Approved for public release; distribution unlimited.

12b. DISTRIBUTION CODE

13. ABSTRACT *(Maximum 200 words)*
We propose an empirical equation to simulate the potential-current and power-current curves for a polymer electrolyte membrane fuel cell (PEMFC) stack. The equation has been demonstrated to fit experimental curves excellently for the entire reaction process, including activation, ohmic, and mass-transfer controls. Using this equation to simulate the mass-transfer process will not cause different results for the E_0, b, and R values than using the analytical equation ($E_i = E_0 - b \log i - Ri$). The effect of each mass-transfer parameter on the shape of the potential-current and power-current curves are compared, and overall they show a regular variation. We also analyzed the effect of relative humidity on the performance of a strip design PEMFC stack.

14. SUBJECT TERMS	15. NUMBER OF PAGES
Nafion, current density, power density, kinetic parameters	16
	16. PRICE CODE

17. SECURITY CLASSIFICATION OF REPORT	18. SECURITY CLASSIFICATION OF THIS PAGE	19. SECURITY CLASSIFICATION OF ABSTRACT	20. LIMITATION OF ABSTRACT
Unclassified	Unclassified	Unclassified	UL

NSN 7540-01-280-5500

Standard Form 298 (Rev. 2-89)
Prescribed by ANSI Std. Z39-18
298-102